

Figure 4 – ST-FNSF/Pilot Plant cross-section.

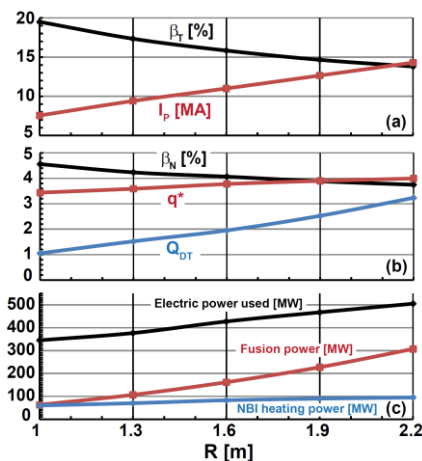


Figure 5 – ST-FNSF parameters vs. R for fixed average neutron wall loading = $1\text{MW}/\text{m}^2$.

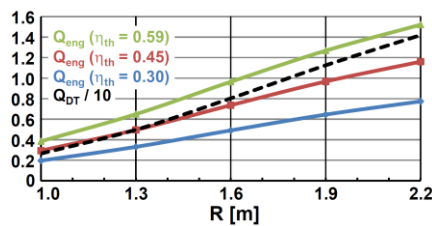


Figure 6 – ST-FNSF engineering gain Q_{eng} and fusion gain Q_{DT} vs. R at fixed $\beta_N = 6$, $q^* = 2.5$.

blanket thermal conversion efficiency $\eta_{\text{th}} = 0.59$ [10]. For $\eta_{\text{th}} = 0.45$, the device size increases to $R=1.9\text{--}2\text{m}$, and still larger devices are required for lower η_{th} . A near-term issue to be addressed is the impact of device size on tritium breeding ratio (TBR) where smaller devices will likely have more difficulty achieving $\text{TBR} > 1$ since a higher fraction of in-vessel surface area must be dedicated to auxiliary heating ports and blanket test modules.

Recent assessments of the divertor heat flux scaling in NSTX project to peak divertor heat fluxes $\geq 20\text{MW}/\text{m}^2$ in the Upgrade for conventional divertor configurations with flux expansion ~ 20 . Very high flux expansions of $\sim 40\text{--}60$ have recently been shown to successfully reduce peak heat flux in NSTX [8], and additional divertor poloidal field coils are being incorporated into the Upgrade design to support high flux expansion "snowflake" [8] and "X/Super-X" [9] divertors and strike point control for high heat flux mitigation while also improving CHI plasma startup capabilities.

For ST-FNSF design, the divertor region is also a critical and challenging area. Figure 4 shows the cross-section of an ST FNSF/Pilot Plant [7] indicating the blanket modules (pink), vacuum vessel (gray), TF coil legs (orange), center-stack (dark orange), divertor PF coils (orange), and superconducting outer PF coils (green). In this unique configuration, the divertor Cu PF coils are placed in the ends of the center-stack to enable high-triangularity plasma shapes with flux expansion of 15-20 compatible with demountable TF legs and a removable center-stack. Design work to incorporate the snowflake divertor in ST-FNSF is underway.

Understanding the impact of varied device size is another important ongoing ST-FNSF research activity. For example, for an ST-FNSF with $A=1.7$, $\kappa=3$, $B_T=3\text{T}$, 500keV NNBI for heating and current drive, $H_{98}=1.2$, $f_{\text{Greenwald}}=0.8$, and average neutron wall loading of $1\text{MW}/\text{m}^2$, Figure 5 shows that as the plasma major radius R is increased from 1m to 2.2m , the impact is stabilizing, since $\beta_T = 19 \rightarrow 14\%$, $\beta_N = 4.5 \rightarrow 3.8$, and $q^* = 3.5 \rightarrow 4.2$. However, the overall fusion power = $60\text{MW} \rightarrow 300\text{MW}$, the tritium consumption also therefore increases by a factor of 5, and the electric power consumed increases from $350\text{MW} \rightarrow 500\text{MW}$. For higher performance operation targeting net electricity production with fixed $B_T=2.6\text{T}$, $H_{98}=1.5$, $\beta_N = 6$, $\beta_T = 35\%$, and $q^* = 2.5$, Figure 6 shows that as R is increased from 1m to 2.2m the smallest possible ST device that can achieve electricity break-even ($Q_{\text{eng}}=1$) has $R=1.6\text{m}$ assuming very high

- [1] M. Peng, et al., Plasma Physics and Controlled Fusion **47** (2005) B263–B283
- [2] M. Peng, et al., Fusion Science and Technology **56** (2009) 957
- [3] G. Voss, et al., Fusion Engineering and Design **83** (2008) 1648–1653
- [4] M. Kotschenreuther, et al., Fusion Engineering and Design **84** (2009) 83–88
- [5] B. Kuteev, et al., Nuclear Fusion **51** (2011) 073013
- [6] V. Chan, et al., Fusion Science and Technology **57** (2010) 66
- [7] J. Menard, et al., Nuclear Fusion **51** (2011) 103014
- [8] V. Soukhanovskii, et al., Nuclear Fusion **51** (2011) 012001
- [9] M. Kotschenreuther, et al., Physics of Plasmas **14** (2007) 072502
- [10] F. Najmabadi, et al., Fusion Engineering and Design **80** (2006) 3–23